Numerical Investigation of High Delta T Sensible Storage Integrated CO2 Heat Pump

Preprint

Ransisi Huang, Nelson James, Eric Kozubal, and Jason Woods

National Renewable Energy Laboratory

Presented at the 20th International Refrigeration and Air Conditioning Conference
West Lafayette, Indiana
July 15 - 18, 2024

NREL is a national laboratory of the U.S. Department of Energy
Office of Energy Efficiency & Renewable Energy
Operated by the Alliance for Sustainable Energy, LLC

This report is available at no cost from the National Renewable Energy Laboratory (NREL) at www.nrel.gov/publications.

Contract No. DE-AC36-08GO28308

Conference Paper
NREL/CP-5500-89702
November 2024

Numerical Investigation of High Delta T Sensible Storage Integrated CO2 Heat Pump

Preprint

Ransisi Huang, Nelson James, Eric Kozubal, and Jason Woods

Suggested Citation
Huang, Ransisi, Nelson James, Eric Kozubal, and Jason Woods. 2024. *Numerical Investigation of High Delta T Sensible Storage Integrated CO2 Heat Pump: Preprint*. Golden, CO: National Renewable Energy Laboratory. NREL/CP-5500-89702. https://www.nrel.gov/docs/fy25osti/89702.pdf.

NREL is a national laboratory of the U.S. Department of Energy
Office of Energy Efficiency & Renewable Energy
Operated by the Alliance for Sustainable Energy, LLC

This report is available at no cost from the National Renewable Energy Laboratory (NREL) at www.nrel.gov/publications.

Contract No. DE-AC36-08GO28308

Conference Paper
NREL/CP-5500-89702
November 2024

National Renewable Energy Laboratory
15013 Denver West Parkway
Golden, CO 80401
303-275-3000 • www.nrel.gov

NOTICE

This work was authored by the National Renewable Energy Laboratory, operated by Alliance for Sustainable Energy, LLC, for the U.S. Department of Energy (DOE) under Contract No. DE-AC36-08GO28308. Funding was provided by the U.S. Department of Energy Office of Energy Efficiency and Renewable Energy Building Technologies Office. The views expressed herein do not necessarily represent the views of the DOE or the U.S. Government. The U.S. Government retains and the publisher, by accepting the article for publication, acknowledges that the U.S. Government retains a nonexclusive, paid-up, irrevocable, worldwide license to publish or reproduce the published form of this work, or allow others to do so, for U.S. Government purposes.

Cover Photos by Dennis Schroeder: (clockwise, left to right) NREL 51934, NREL 45897, NREL 42160, NREL 45891, NREL 48097, NREL 46526.

NREL prints on paper that contains recycled content.

Numerical investigation of high delta T sensible storage integrated CO2 heat pump

Ransisi HUANG[1], Nelson James[1], Eric Kozubal[1], Jason WOODS[1]*

[1]National Renewable Energy Laboratory, Building Technology Science Center

Golden, Colorado, United States

* Corresponding Author: Jason.Woods@nrel.gov

ABSTRACT

To assist building heating electrification, this paper numerically investigates a load flexible heat pump system for commercial buildings. The system consists of a CO_2 vapor compression cycle, a sensible thermal storage tank, and an air handling unit. The thermal storage medium is inexpensive, non-toxic and stable anti-freeze solution (30% potassium acetate). The air handling unit has an indoor coil and a ventilation coil. The system can be used to manage building electric load. During peak hours, the heat pump is off, and the hot solution water is discharged from the tank to heat up the indoor air and ventilation air. During the hour of charge, the heat pump delivers hot solution water to the tank and to the air. The tank can also stand by while the heat pump provides space heating directly.

We selected a medium sized office building located in Minnesota as the representative building and used EnergyPlus to obtain its 24-hour load data. We designed three storage tank volumes assuming 50°C, 65°C and 80°C tank temperatures to independently provide the building load for 4 hours in the morning. The higher the tank temperature, the smaller the required volume, and thus higher energy density. The effective energy density is 78 kWh_{th}/m^3 with an 80°C tank, and 40 kWh_{th}/m^3 with 50°C.

We simulated the tank integrated heat pump performance subjected to the 24-hour building load profile and ambient data. The baseline is the same system without storage tank. There was a trade-off between the storage energy density and the charging COP. The charge hour COP was 2.77 to charge the tank to 80°C, and 3.01 to 50°C. The proposed system could shift building load from the peak hours (8:00 – 12:00) to off-business hour (23:00 – $7:00^{+1}$). It eliminated 100% compressor electricity use during the peak hours and avoided a peak electric power of 34 kW. The 65°C tank saved 9.5 kWh_e (4%) considering all day operation, which was the best balance between energy density and the system operation efficiency among the three options.

1. Introduction

In the United States, the building sector accounts for about 40% of greenhouse gas emissions, and heating, ventilating, and air conditioning (HVAC) accounts for about 35% of building energy (DOE, 2015). These numbers present critical opportunities to decarbonize building energy systems. Electrifying the building space heating by replacing fossil fuel boilers with high efficiency electric heat pumps has been investigated by researchers worldwide. Thomaben et al. (2021) found that heat electrification in EU can reduce the total energy related emissions by up to 17%. Nadel and Perry (2020) found that heat electrification in the U.S. commercial sector could reduce commercial building energy related emissions by 44%. The greenhouse gas emission reduction is predicted to be 38-53% in U.S. residential sector (Vaishnav and Fatimah, 2020).

On the other hand, most literatures conclude that shifting to heat pumps would bring a strong impact on the existing grid. Vaishnav and Fatimah (2020) found that wide deployment of heat pump in U.S. would increase annual hourly peak demand for electricity, and would shift peak demand from summer to winter for some locations. Similarly, Milev et al. (2023) found that U.K. would see a 144% increase in total daily demand of electricity relative to the present grid level. Wu et al. (2022) found that the heating electricity demand of two major cities in the northern China alone would exceed 20% of the current total social electricity consumption. They suggest the development of auxiliary energy storage facilities to support the wide implementation of heating electrification.

Thermal energy storage (TES) can help alleviate the impact on the grid by shifting thermal load and reducing the peak demand of electricity in buildings. Thermal storage can be sensible, latent or thermo-chemical. Among the three options, sensible storage is the most economical viable option and has the best potential for large scale implementation. There exists quite some research on integrating a sensible tank with vapor compression heat pumps. Bakirci and Yuksel (2021) experimentally and theoretically studied a solar-source heat pump with a storage tank in Turkey. They reported the whole system COP between 2.3 – 3.3, with outdoor temperature varying between -2.8°C to 12.2°C. Sifnaios et al. (2019) investigated a stratified water tank connected to a heat pump via a validated CFD model. They

found that higher degree of stratification leads to higher COP. Wu et al. (2022) field tested an air-source heat pump with a storage tank that was installed in a single-family building in Beijing. The tank was charged by the heat pump in the daytime and discharged at night. They reported a seasonal COP of 2.95 with the ambient temperature varying between -9.3°C to 11.3°C.

We identified three limitations from the current literature. First, the previous study normally considered heat pumps with high GWP refrigerants (e.g. R134a, R410A). Second, system performance of a storage tank integrated heat pump under cold climate conditions (< -10 °C) was not much evaluated. Third, most previous studies focused on characterizing the equipment operating efficiency (COP or seasonal COP) assuming residential applications. However, according to Nadel and Perry (2020), the commercial sector presents an equally significant decarbonization potential as the residential sector, with load characteristics very distinct from residential buildings.

Motivated by the need to transition to natural refrigerants and to decrease the carbon footprint associated with commercial sector space heating, we propose a load flexible CO_2 heat pump with a sensible storage tank for commercial buildings with significant ventilation load. The thermal storage medium is 30% potassium acetate solution. We used a medium sized office building located in Minnesota as the representative building. We first designed three storage tank volumes assuming 50°C, 65°C, and 80°C tank supply temperatures to meet the building load for 4 hour in the morning. We then simulated the performance of the proposed system subjected to the 24-hour building load data and the ambient weather data in Minnesota. The system performance was compared to that of a baseline, which is the same heat pump system without storage.

2. Methodology

2.1 System description

Figure 1 shows the schematic of the sensible storage integrated heat pump system. It consists of a CO_2 vapor compression refrigerant circuit and a 30% potassium acetate (KAc) solution loop. The KAc solution serves as both thermal storage medium and the heat transfer fluid that circulates between the tank (or gas cooler) and the air handling unit (indoor coil and ventilation coil). As shown in the figure, the system has three operating modes. 1) Discharge mode. The compressor is turned off, and the tank discharges hot solution to the air handling unit. The solution flows through the indoor coil first to heat up the return air, and then heats up the ventilation air. This sequence allows the air handling unit to extract solution heat to the largest extent. After being fully exhausted, the cold solution from the ventilation coil returns to the bottom of the tank and creates thermal stratification in the tank. 2) Hybrid charge mode. the heat pump delivers the hot solution to both the tank and the air handing unit, charging the thermal storage while providing the building load and the ventilation load. 3) Tank stands-by mode. The tank is bypassed, and the heat pump directly provides hot solution to meet the required heating load.

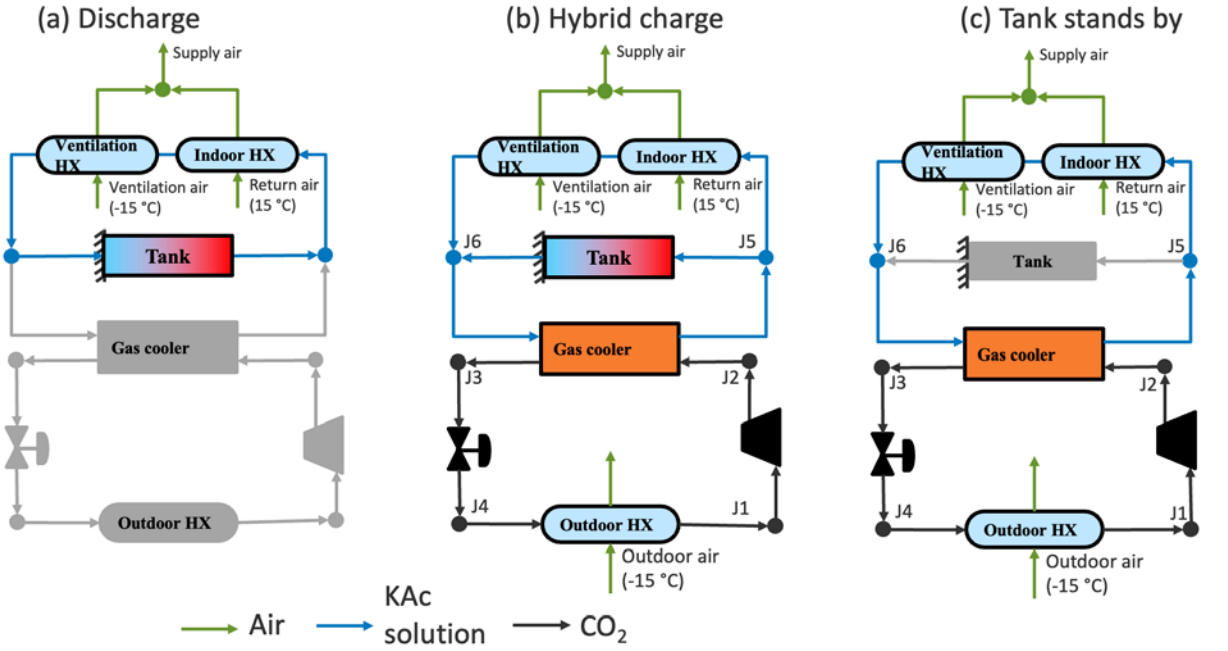

Figure 1 Schematic of the sensible storage tank integrated CO_2 heat pump. (a) discharge mode; (b) hybrid charge mode; (c) tank stand-by mode

The system was simulated with a quasi-steady state component-based framework. The outdoor coil was modeled with a two-zone approach. The heat transfer in each zone was characterized by a lumped heat transfer coefficient. The indoor coil and ventilation coil were modeled with an effectiveness-NTU approach. The gas cooler was modeled with segment-by-segment LMTD approach. Due to the lack of variable speed CO_2 compressor map at trans-critical operation, we assumed that both volumetric efficiency and the isentropic efficiency were a linear function of the compression ratio. The following assumptions are used for the system simulation:

- All components except for the tank are assumed at steady-state operation
- Expansion devices are represented with an isenthalpic process
- Pressure drops are neglected in all heat exchangers
- Power consumptions of the fans and pumps are neglected
- Heat loss through the tank wall to the ambient is neglected

2.2 Stratified tank

A one-dimensional, multi-node tank model was developed to predict the performance of the anti-freeze based sensible thermal storage during discharging and charging. Figure 2 shows the schematic of the stratified tank model. During charge, solution is pulled from bottom node *c* to be sent to the gas cooler. Hot solution supplied from the gas cooler is sent to node *a* based on the returning fluid density. During discharge, solution is pulled from node *b* (to be sent to the air handing unit) based on the position of the dip tube. Cold solution returning from the air handing unit is sent to the bottom node *c*. Conduction as well as advection driven heat and mass transfer alter the temperature and density of intermediate nodes.

As shown in the figure, the tank is divided into multiple segments called nodes. Each node in the model had a fixed position in space. The temperature and mass within each node are assumed constant during each timestep of the model. Mass and energy balances calculations are performed over each node to determine changes in mass and temperature with respect to time. These time derivatives are then used to update the temperature and mass of each node after each timestep. The model assumed that the tank was vented to atmosphere and the liquid level within the tank varied as the fluid thermally expanded and contracted. The top node was allowed to be partially filled to account for the changing liquid level in the tank. As the liquid level rose, additional nodes were included in the calculations. Similarly, as the liquid level dropped nodes were removed from consideration in the calculations. Thermodynamic properties of the potassium acetate mixture were taken from literature (Tanaka et al., 2015).

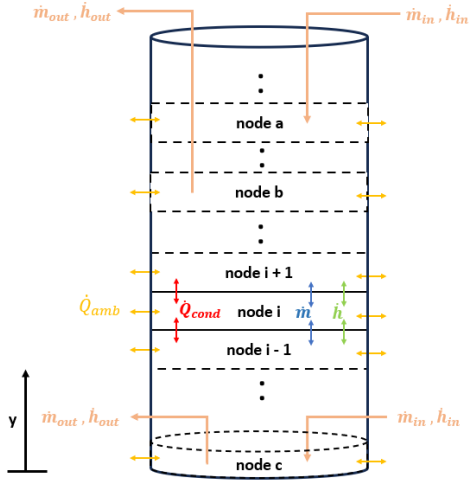

Figure 2 Schematic of the modeled stratified storage tank

For each timestep in the model the temperatures and mass flow rates of fluid entering and leaving the tank were specified. Equations (*1*) – (6) were used to determine each node's mass and temperature change with respect to time. Assuming an incompressible liquid, the volume of fluid entering a node must equal the volume of fluid exiting a node. The change in mass of each node with respect to time was calculated as a sum of volume flows multiplied by the respective density of the volumes entering and leaving the node, Equation (*1*).

$$\frac{dm}{dt}_i = \dot{V}_{in}\,\rho_{in} - \dot{V}_{out}\rho_i = \dot{m}_{in} - \dot{m}_{out} \qquad (1)$$

The change in temperature with time of a particular node due to heat conduction between nodes and heat conduction perpendicular to the tank wall was determined using Equation (2).

$$\frac{dT}{dt}_{cond,i} = \frac{U\,A_{side}}{m_i\,c_{p,i}}(T_i - T_{amb}) + \frac{k_i\,A_{base}}{\frac{\Delta y}{2}\,m_i\,c_{p,i}}\,(T_{i+1} - 2T_i + T_{i-1}) \quad (2)$$

For nodes where fluid was entering or leaving the tank, the temperature change with respect to time was given by Equations (3) and (4). Depending on the location of a node relative to the inflow and outflow nodes, the net advective flow of fluid was calculated using a mass balance. This flow was used to determine the node's advection driven temperature change with respect to time using Equation (5) where h_{in} represents the enthalpy of the adjacent node in the direction of the advection flow entering the node. The total temperature change of a node after each time step was taken as the sum of the temperature change contributions from conduction, inflow and outflow of ports, and advection as shown in Equation (6).

$$\frac{dT}{dt}_{port_{in}\ i} = \frac{\dot{m}_{port_{in}} h_{in}}{m_i c_{p_i}} \quad (3)$$

$$\frac{dT}{dt}_{port_{out}\ i} = \frac{\dot{m}_{port_{out}} h_i}{m_i c_{p_i}} \quad (4)$$

$$\frac{dT}{dt}_{advec\ i} = \frac{\dot{m}_{in}\,h_{in} - \dot{m}_{out} h_i}{m_i c_{p_i}} \quad (5)$$

$$\frac{dT}{dt}_i = \frac{dT}{dt}_{cond,i} + \frac{dT}{dt}_{port_{in}\ i} + \frac{dT}{dt}_{port_{out}\ i} + \frac{dT}{dt}_{advec\ i} \quad (6)$$

2.3 Building load characteristics

A potential application for the heat pump is a commercial building that is designed with mechanical ventilation. We used a medium sized office building located in Minnesota as the representative building to evaluate the performance of the proposed heat pump system with sensible storage. The building model was based on ASHRAE 90.1 – 2013 DOE prototype commercial building model (Building Energy Codes Programs, 2023). EnergyPlus was used to predict the 24-hour internal and ventilation loads for the building. The ambient temperature ranges between -14°C and -18°C, and the maximum building load (including internal and ventilation load) was 94 kW. The building load profile is shown in Figure 3. The indoor air temperature control in the reference building model is not ideal as the morning setpoint is below the typical comfort levels for the building occupants (outside the ASHRAE comfort zone). Despite this, we believe the building model can still provide insight into the impacts of various tank supply temperatures on the thermal load shifting performance. The building model utilized natural gas heating as a default. To generate a baseline for the proposed system, the same CO_2 heat pump without storage tank was assumed to provide the heat that was generated by the gas-powered rooftop unit.

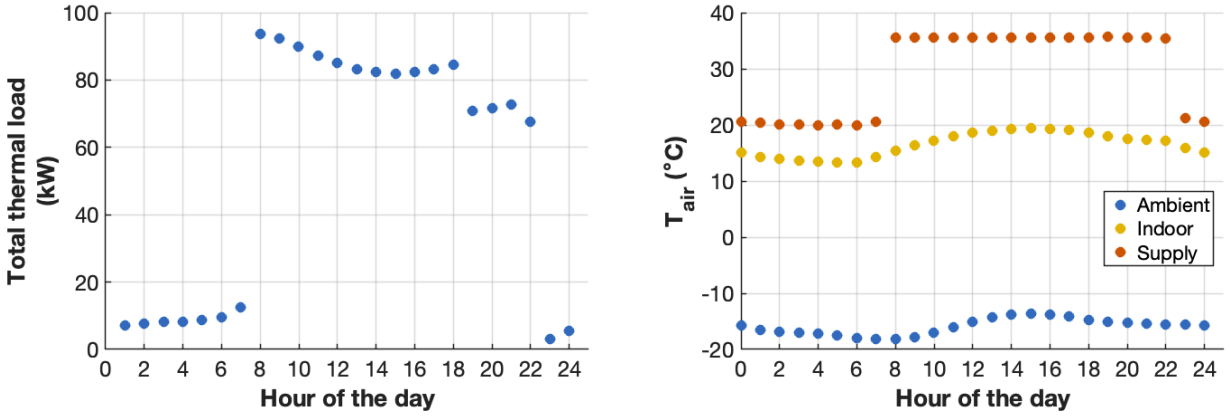

Figure 3 24-hour profile of the (left) total building thermal load and (right) ambient temperature, indoor temperature, and supply air temperature

2.4 Peak shaving operation

The system is controlled to alternate among the three operating modes to shift the electric building load. We implemented a schedule-based peak shaving strategy. As shown in Table 1, the discharge window is set from 8am – 12pm to coincide with the high demand at the beginning of the building business hours. In this window, the compressor is turned off to reduce the electricity use. Depending on the hot solution water discharged from the tank, the system

varies solution flow rate to meet the indoor setpoint. The charge window is set across the non-business hours from 11pm to 7am when the ventilation load was low due to low occupancy. In this window, the system controls the tank charging rate and meets the indoor setpoint by varying the flow rate allocated to the tank and to the air handling unit, respectively. For the other time of the day, the tank was bypassed.

Table 1 System operation modes

Time window	Tank operation mode	Heat pump operation
8:00 – 12:00	Discharge	Tank provides space heating with heat pump off
12:00 – 23:00,	Stand-by	Heat pump provides space heating
23:00 – 7:00^{+1}	Charge	Heat pump simultaneously charges the tank and provides space heating
7:00^{+1} – 8:00^{+1}	Stand-by	Heat pump provides space heating

3. Results and Discussion

3.1 Tank design

We aim to design the tank such that the stored energy can sustain the building load for 4 hours (8:00 – 12:00) on the design day, which, based on the building load characteristics, is equivalent to an energy capacity of 359 kWh_{th}. The most critical design parameters are the volume and the tank supply temperature. Figure 4 shows the temperature supplied from the tank to the air handling unit as a function of time for three different tank volumes. Because the tank is thermally stratified, the supply temperature drops significantly toward the end of the discharge. The smaller the tank, the sooner the tank supply temperature reaches the cut-off temperature, which is the lowest temperature that can heat the air to the desired supply temperature (35°C). As shown in the figure, a tank of 6.1 m^3 or 6.8 m^3 can sustain for 4 hours, while the volume of 5.3 m^3 will cause a cut-off prior to 12:00.

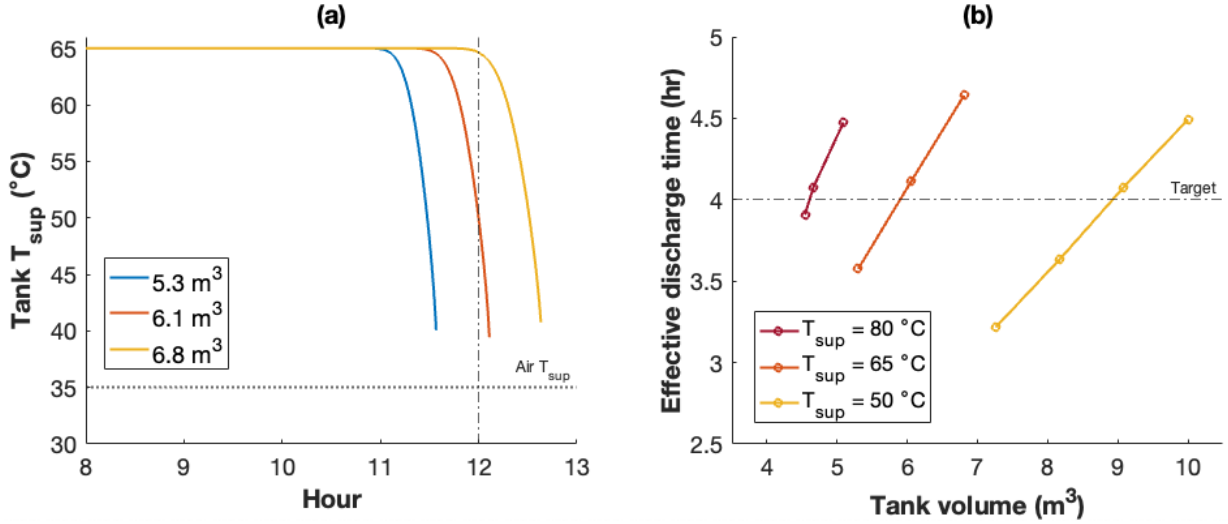

Figure 4 (a) Tank supply temperature profiles at different tank volumes; (b) Effect of tank volume and tank initial supply temperature (T_{sup}) on effective discharge time

Figure 4 (b) shows the effect of the tank volume and the tank supply temperature on the effective discharge hours, with a total of 4 hours being the design target. With the same initial supply temperature, the larger the tank, the longer the discharge hours. On the other hand, increasing the initial supply temperature reduces the tank volume required to reach similar discharge hours, and thus increases the energy density (ratio of energy capacity over volume). For each tank supply temperature, we chose the smallest tank volume that still meets the 4-hour discharge goal. Table 2 shows the three tanks that we designed to provide 4-hour discharge.

Table 2 Design of the tank volumes with three different tank supply temperatures

Tank T_{sup} (°C)	Volume (m^3)	Effective energy capacity (kWh_{th})	Effective energy density (kWh_{th}/m^3)
80	4.7	365.7	78.5
65	6.1	368.6	60.8
50	9.1	365.0	40.2

3.2 System operation characteristics

For this section, we use the system simulation with 80°C tank supply temperature to illustrate the operation characteristics. Figure 5 shows the progression of the tank temperature distribution along the tank height direction. At the onset of discharge operation (8:00), the tank was isothermally at 80°C. The air handling unit drew the hot solution from the top of the tank and returned cold solution (at -10°C) to its bottom, creating the thermoclines as shown in (a). At the end of the discharge window (12:00), the tank has run out of 80°C hot solution, with over half of the tank filled with cold solution at -10°C. During charge operation (starting from 23:00), the gas cooler of the heat pump drew cold solution from the bottom of the tank and heated it up to 80°C before dropping it to the top of the tank. The thermocline moved from the top to the bottom of the tank, as the heat pump restored the hot solution in the tank. At 6:43AM, the temperature at the bottom of the tank has been restored to 45°C, and the heat pump stopped charging due to the cycle thermodynamic limit.

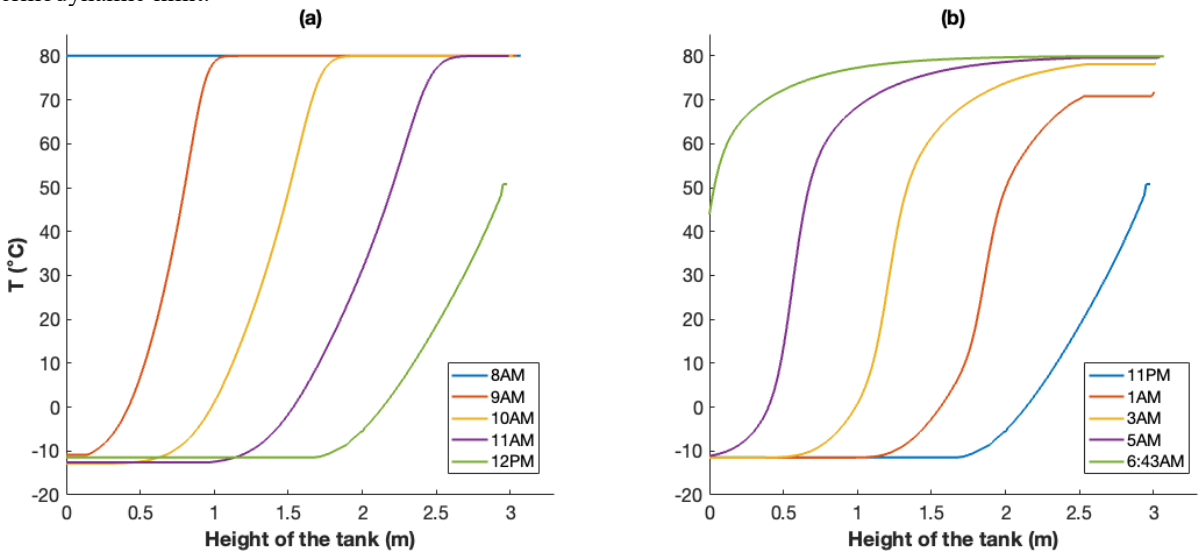

Figure 5 Snapshots of tank temperature distribution along the tank height over (a) discharge window and (b) charge window, with initial tank temperature at 80°C

Figure 6 shows the vapor compression heat pump system operations during the charging window on a P-h and a T-s diagram. The cycle enjoyed a small throttling loss, because the solution from the bottom of the tank was cold enough to bring down the temperature at J3 (gas cooler outlet). As the tank thermocline moved toward the tank bottom, the solution temperature returning to the gas cooler increased, raising the temperature at J3 and moving J4 (evaporator inlet) toward higher quality. The quality at J4 was very high (>0.5) when the tank charging was approaching the end, posing challenge for heat pump operation. The system terminated the charging operation when the quality at J4 exceeded 0.75, or COP dropped below 50% of that at the start of charging, whichever came first. Another challenge associated with providing 80°C hot solution is that the compressor discharge temperature (T at J2) exceeded 130°C over the entire charge window and exceeded 160°C at the end. This indicates the system is unlikely to operate at the end of the charging window.

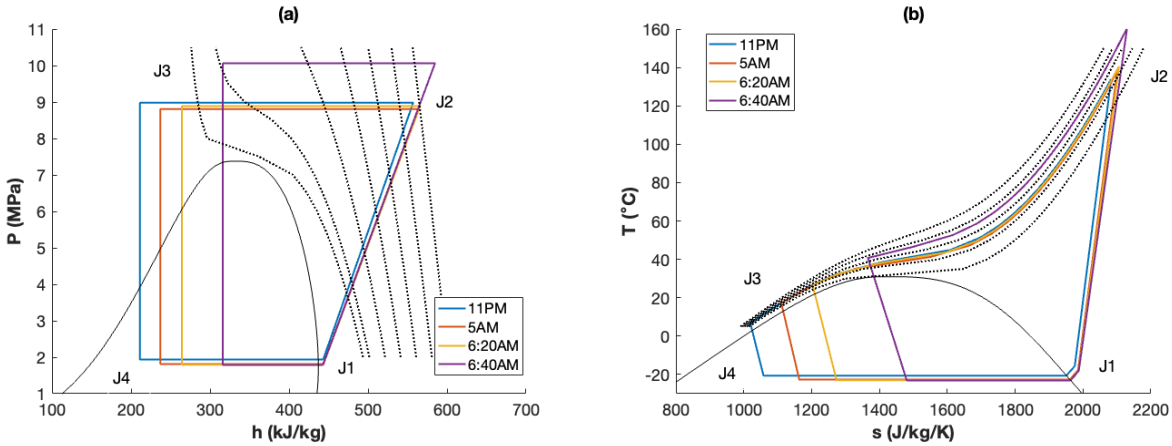

Figure 6 Vapor compression system solutions over the charge window on the (a) P-h diagram and (b) T-s diagram, with a charging temperature of 80 °C

The system charging operation is greatly impacted by the tank supply temperature. The higher the tank supply temperature, the higher the pressure lift during charging operation, and thus lower COP. On the other hand, higher tank supply temperature helps reduce the tank volume, and thus increases the effective energy density. Figure 7 shows the charge window COP as a function of the tank effective energy density. 80°C tank supply temperature results in the highest energy density (78 kWh/m^3) but the lowest charging COP. Reducing the supply temperature from 80°C to 65°C results in a 23% reduction in energy density and 7% increase in charging COP. Reducing from 65°C to 50°C results in a 34% decrease in energy density, but only 1% increase in charging COP.

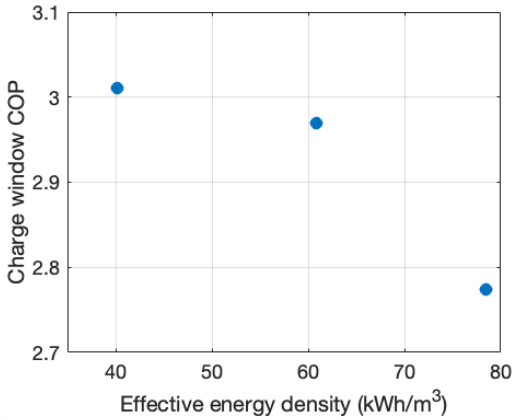

Figure 7 System charging COP as a function of effective energy density. The three points from left to right indicate 50°C, 65°C, and 80°C tank supply temperature

3.3 System peak shaving performance

Figure 8 shows how the integrated system shifts the thermal load from the morning (that sees the maximal building load) to the night (that sees the minimal load due to low human occupancy). The heat pump was off from 8:00 to 12:00, and the stored sensible energy was discharged from the tank to meet the building load. After being fully exhausted, the tank was bypassed while the heat pump was turned on to meet the building load. From 23:00 to 7:00^{+1}, the heat pump was operated to restore the hot solution in the tank while meeting the miniscule building load. At all times, the heat rate provided by the air handing unit (indoor and ventilation coil) matched the total building thermal demand including the ventilation and internal load.

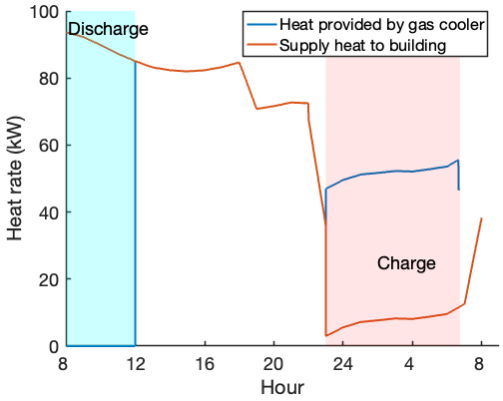

Figure 8 Heat rate profile of the storage tank integrated CO_2 heat pump

Figure 9 compares the electric power and energy use of the integrated system against the baseline, where the tank was always in stand-by mode. Not surprisingly, the integrated system avoided electricity use over the 4-hour discharge window that would otherwise be subjected to high compressor power. During the charge window, the building load was as low as 5% of the system design capacity, posing a capacity modulation challenge to the heat pump operation. To overcome the mismatch between the load and the designed capacity, the baseline system had to significantly ramp down the compressor speed and operate with runtime fraction less than 1. The cyclic degradation resulting from this part time operation was not simulated in the current study. Charging the tank allows the heat pump to take advantage of this period and operate continuously. Figure 9 (b) compares the accumulative electricity use, which shows that the peak shaving case was nearly energy-neutral comparing to the baseline case at the end of charge window.

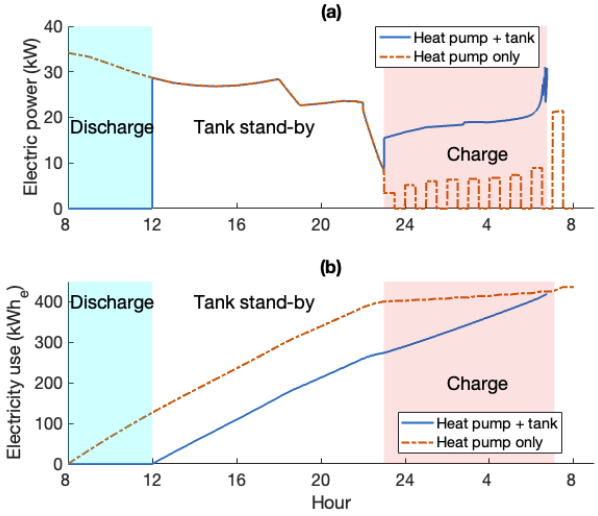

Figure 9 CO_2 heat pump power and energy performance with and without storage tank: (a) compressor electric power profile; (b) compressor electricity consumption profile. Charging temperature to tank is 80°C

It is worth noting that with the current system design and charging operation, it is unlikely to fully charge the tank. The heat pump only charged 340 kWh_{th} into the tank before the system hit the charging termination criterion, while fully restoring the tank to isothermally 80°C requires 359 kWh_{th}. There exists a couple of options to charge the last ~20 kWh_{th} into the tank. We may draw on the electric heating to continue charging the tank after the heat pump stops charging, although this is unlikely an energy efficient approach. Alternatively, we can explore different system layouts that introduce an additional heat sink to help bring down the solution temperature into the gas cooler, when the temperature at the tank bottom becomes too high. In any case, such investigation is beyond the scope of this paper. For simplicity, we will just subtract the uncharged energy from the effective energy capacity of the tank, meaning the tank will reach cut-off threshold sooner than the designed condition.

With this assumption, Table 3 shows the breakdown of the electricity use in discharge and charge windows. With 80°C tank supply temperature, using the tank for peak shaving was energy-neutral comparing to the baseline. With 65°C supply temperature, the tank saved 9.5 kWh_e over the drive cycle operation. Further reducing the temperature

to 50°C did not bring much improvement on the electricity savings. Therefore, among the three supply temperatures that we investigated, 65°C strikes the best balance between storage energy density and system operation performance.

Table 3 Electricity use breakdown of the heat pump system with and without storage tank

Tank supply T	Operation window	Electricity use, heat pump only (kWh_e)	Electricity use, heat pump + tank (kWh_e)	Electricity use saving (kWh_e)
80°C	8AM – 12PM (Discharge)	119.9	0	119.9
	11PM – 7AM^{+1} (Charge)	25.2	145.2	-120.0
	Drive cycle	145.2	145.2	-0.1
65°C	8AM – 12PM (Discharge)	121.2	0	121.2
	11PM – 7AM^{+1} (Charge)	25.2	136.9	-111.7
	Drive cycle	146.4	136.9	9.5
50°C	8AM – 12PM (Discharge)	122.0	0	122.0
	11PM – 7AM^{+1} (Charge)	25.2	135.8	-110.6
	Drive cycle	147.2	135.8	11.4

4. Conclusions

We numerically investigated a load flexible CO_2 heat pump system that can shave peak electric load of building space heating. A storage tank and air handling unit are connected to the gas cooler in parallel via a secondary loop that circulates 30% KAc solution. The system can operate in 3 modes: discharge, hybrid charge and tank standby. The heat pump charges the storage tank by adding hot solution water to the top of the tank. Depending on the operating mode, the hot solution discharged from the tank (or supplied by the gas cooler) sequentially heats up the building return air and the ventilation air (cold ambient air). We obtained a winter daily profile of a commercial building with mechanical ventilation that is located in MN. We designed three storage tank volumes assuming 50°C, 65°C, 80°C tank temperatures to shave 100% compressor electric load for 4 hours in a winter morning, which corresponds to a total energy capacity of 359 kWh_{th}. We evaluated the heat pump performance with the three tanks subjected to the 24-hour building data profile. The baseline is the same system without storage tank. Main conclusions are as follows:

- The higher the tank supply temperature, the smaller the required volume, and thus higher energy density. With 80°C tank temperature, the effective energy density of the storage tank is 78 kWh_{th}/m^3. With a 50°C tank, the energy density is 40 kWh_{th}/m^3.
- There is a trade-off between the storage energy density and the charge hour COP. Higher tank temperature results in higher energy density, but also increases the compressor power during the charge hours. The overall charge COP is 2.77 with an 80°C tank, and 3.01 with a 50°C tank. Also, charging the tank to 80°C results in high discharge temperature, posing challenge to reliable compressor operation.
- It is overall difficult for the heat pump to charge the last 6% capacity of the tank and fully restore the tank to the initial isothermal state. When the temperature at the bottom of the tank is raised to over 50°C, the CO_2 cycle suffers from large throttling loss, with the quality entering the evaporator exceeding 0.6.
- With properly sized tanks, the integrated system can shift building load from the morning (8:00 – 12:00) to the night (23:00 – 7:00^{+1}). While the baseline system without storage tank suffers from drastic mismatch between the miniscule off-business building load and the designed system capacity, charging the tank at night ensures continuous heat pump operation.
- Comparing to the baseline, the sensible storage eliminates all the compressor electricity use during discharge window, which is about 120 kWh_e, and avoids 34 kW electric power. The electricity saving over 24 hours depends on the designed tank temperature. A 65°C tank saves 9.5 kWh_e (4%) considering all day operation, which is the best balance between energy density and the system operation efficiency.

NOMENCLATURE

A	area	(m^2)
c_p	specific heat capacity	(J/K-kg)
h	enthalpy	(J/kg)
m	mass	(kg)
$\dot{m}$	mass flow rate	(kg/s)
P	pressure	(Pa)
T	temperature	(K)
U	heat transfer coefficient	(W/m^2-K)
$\dot{V}$	volumetric flow rate	(m^3/s)
x	quality	(-)
ρ	density	(kg/m^3)

Subscript

advec	advection related
cond	heat conduction related
in	inlet
out	outlet
sup	supply

REFERENCES

Building Energy Codes Programs (2023). Prototype Building Models. U.S. Department of Energy Office of Energy Efficiency and Renewable Energy. https://www.energycodes.gov/prototype-building-models

Bakirci, K., & Yuksel, B. (2021). Simulation study of solar-source heat pump system with sensible energy storage. Journal of Thermal Analysis and Calorimetry, 146, 1853-1864.

Doe, U. (2015). An assessment of energy technologies and research opportunities. Quadrennial Technology Review. United States Department of Energy, 12-19.

Milev, G., Al-Habaibeh, A., Fanshawe, S., & Siena, F. L. (2023). Investigating the effect of the defrost cycles of air-source heat pumps on their electricity demand in residential buildings. Energy and Buildings, 300, 113656.

Nadel, S., & Perry, C. H. R. I. S. (2020). Electrifying space heating in existing commercial buildings: opportunities and challenges. American Council for an Energy-Efficient Economy (ACEEE) Publication.

Sifnaios, I., Fan, J., Olsen, L., Madsen, C., & Furbo, S. (2019). Optimization of the coefficient of performance of a heat pump with an integrated storage tank–A computational fluid dynamics study. Applied Thermal Engineering, 160, 114014.

Tanaka S., Ogawa K. and Sasaki N. (2015), Fundamental Properties of Potassium Acetate Aqueous Solutions, Netsu Bussei, 29(3), 129-134.

Thomaßen, G., Kavvadias, K., & Navarro, J. P. J. (2021). The decarbonisation of the EU heating sector through electrification: A parametric analysis. Energy Policy, 148, 111929.

Vaishnav, P., & Fatimah, A. M. (2020). The environmental consequences of electrifying space heating. Environmental Science & Technology, 54(16), 9814-9823.

Wu, P., Wang, Z., Li, X., Xu, Z., Yang, Y., & Yang, Q. (2020). Energy-saving analysis of air source heat pump integrated with a water storage tank for heating applications. Building and Environment, 180, 107029.

Wu, C., Chen, Z., Qin, C., Zhang, Y., & Zhang, X. (2022). Exploring the challenges of residential space heating electrification in China: A case study in Jinan and Qingdao. Case Studies in Thermal Engineering, 37, 102283.

ACKNOWLEDGEMENT

This work was authored by the National Renewable Energy Laboratory, operated by Alliance for Sustainable Energy, LLC, for the U.S. Department of Energy (DOE) under Contract No. DE-AC36-08GO28308. Funding was provided by the U.S. Department of Energy Office of Energy Efficiency and Renewable Energy Building Technologies Office. The views expressed in the article do not necessarily represent the views of the DOE or the U.S. Government. The U.S. Government retains and the publisher, by accepting the article for publication, acknowledges that the U.S. Government retains a nonexclusive, paid-up, irrevocable, worldwide license to publish or reproduce the published form of this work or allow others to do so, for U.S. Government purposes.